

Study on surface settlement of Jinchuan copper-nickel area in time series InSAR

Surface settlement problem in Jinchuan copper-nickel mine area, this paper applies SBAS-InSAR technology and time series D-InSAR technology, and uses multi-temporal Sentinel-1A interference image to study the ground settlement in this area. Timing D-InSAR technology and SBAS-InSAR technology are used for monitoring. After two results comparison and verification analysis, there are two obvious settlement funnels in the mining area, namely 5-7 rows and old pits in the West 2 mining area, and the maximum settlement rate in the 5-7 rows in the West 2 mining area is -13mm/year. The maximum line shape of the radar line of sight is 13mm, and the settlement area reaches 0.45km². There is obvious settlement in the southeast of the old pit. The maximum rate of settlement is -85mm/year, and the maximum line shape of the radar line of sight is 78mm. The settlement area has reached 1.4km² provides an important basis for the safe production of Jinchuan copper-nickel mine.

Keywords: timing D-InSAR; SBAS-InSAR; Sentinel-1A; surface subsidence.

Introduction

The Jinchuan copper-nickel mining area is located in the southern marginal uplift of the Alashan block in the geotectonic position, the inner part of the block in the north, and the edge of the Caledonian trough in the north of the Qilian Mountains. This orebody is mined by a bottomless column caving mining method, which accelerates surface subsidence and ground fissure when firing. Underground mining causes movement and deformation of rock formations and surface, and induces various geological disasters [1]. Therefore, mastering the law of surface deformation can effectively guarantee the safety of people's lives and property, the sustainable development of the national economy and social stability, and has important guiding significance for mine disaster warning and mining subsidence control and governance.

Affected by underground mining activities, the surface subsidence of the mining area is a long-term process with

complex topographic and geological conditions and fast settlement speed, which leads to traditional surface deformation monitoring such as GPS measurement, geodetic levelling and total station measurement in mining area settlement monitoring. There are many problems. First, industrial mining will take a lot of cannon mining methods, resulting in problems in the stability of the standard point, plus mining is a long-term process, the traditional measurement cycle is long, the workload is large, time-consuming and labour-intensive [2]; second, the tradition of the monitoring method only obtains the settlement information locally, which is not conducive to reflecting the settlement law of the whole mining area [3]. Third, the geographical limitation, the traditional measurement needs to know the settlement position in advance to arrange the observation point. Interferometric Synthetic Aperture Radar (InSAR) measurement technology is a space-to-earth observation technology developed rapidly in the past 30 years. It acquires surface change information based on phase information of synthetic aperture radar complex image and can be used to monitor centimeter level. Or a smaller earth surface deformation [4]. Compared to traditional measurement techniques such as visible light and infrared remote sensing, this technology has the advantages of wide coverage, high precision, no weather conditions, and high spatial sampling density. At present, this technology has been widely used in regional surface deformation monitoring [5], hidden point detection [6], glacier freezing and thawing monitoring [7], and flood submerged area change monitoring [8].

On the basis of InSAR technology, in order to obtain high-precision deformation results in mine monitoring, domestic and foreign scholars have carried out a lot of research. In 1993, Massonnet Didier et al. [9] used the SAR image of the ERS-1 satellite to monitor the motion generated by the Landes earthquake in California. The accuracy of the monitoring was higher than that of the previous spatial imaging technique, which was better than 3 cm. Tomás R et al. [10] used DInSAR technology to monitor the settlement of the ground around the Segura river from 1993 to 1995. The study found that some areas settled to 8 cm, which has a guiding effect on predicting and controlling land subsidence in this area. In 2010, Herrera G et al. [11] used coherent pixel technology (CPT) to map and

Messrs. Li Qiang, Wang Weihong, Yang Ning, Han Dan, Zhou Wentao, Southwest University of Science and Technology

monitor the ground motion of the La Union mine, demonstrating that this method can be used for most ground motion in this abandoned mine. In 2014, SayginAbdikan et al. [12] analyzed the defects of D-InSAR and used PS-InSAR technology to monitor the coal mining subsidence area in the northwestern part of Turkey, which fully demonstrated the guiding significance of PS-InSAR technology in mining settlement monitoring. In 2017, Zhu Jianjun et al. [13] focused on the classification of InSAR monitoring methods, analyzed PSInSAR, SBAS-InSAR, and D-InSAR. Finally, it was proposed that these improved interferometric techniques can be used

for settlement monitoring in mining areas; 2018 Li Da et al. [14] used SBAS-InSAR technology to monitor the surface subsidence of the northwestern part of a mining area in Yulin City, Shaanxi province, which proved the reliability of SBAS-InSAR technology in mine settlement monitoring and provided a new means for monitoring the surface subsidence of mining areas. In 2019, Huang Changjun et al. [15] used continuous scattering interferometry (PSI) to illustrate that this method is a useful tool for measuring subsidence in mining areas, overcoming the limitations of traditional interferometry, and the results reveal the evolution of mining subsidence in Geting coal mine, Shandong province. The process provides an early warning to mine disasters.

1. Research area and data overview

The Jinchuan nickel copper mine is located in the northwest of Gansu province. The Jinchuan nickel mine was completed and put into operation in the 1960s. It is the main production base of platinum group metals in China. The West Second Mining Area of Longshou mine is located in the northwest of Gansu province. It is the west of the Yankuang Mining Area. The faults in the mine are developed. The F8 fault is the largest, and the breccia layer is 20~40m thick. The 4 lines of exploration directly contact the orebody, and the geology of the environment is complex and put into production in 1960s. The study area is located in the central part of Jinchang city. The geographical range of the study area is E102.1196~E102.5180, N38.4867~N38.5180, and the total area is about 14 square kilometers. In the study area, there was a clear ground fissure in 2016, and then it was discontinued until the end of 2018.

This paper uses the Sentinel -1A derailment image from January 2018 to November 2018 and the simultaneous discontinuous uplift image to monitor the settlement of the West Second Mining Area. All images are of wide single-view multiple image data (slc), the image coverage is shown in

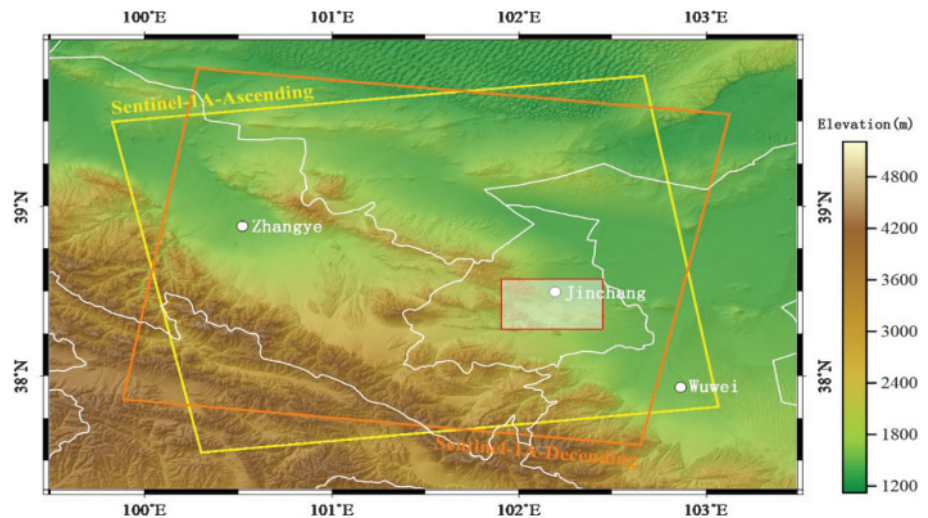


Fig.1 Schematic diagram of satellite coverage of Sentinel-1A radar in Jinchang city

Fig.1, the slant range and azimuth resolution are 3.7 and 22.7m, and the single scene image coverage is about 251km × 251km. A total of 28 scenes of c-band down-track images and 26 scenes of c-band up-track images were used. In order to eliminate the terrain phase in the interference phase, SRTM DEM data with a ground resolution of 30 m was used.

2. Data processing

2.1 BASIC PRINCIPLES OF SBAS-InSAR AND D-InSAR

The basic principle of the SBAS-InSAR (small baseline set) technique is to group a set of SAR complex images over a long time sequence according to certain baseline constraints, and to improve the interferogram's coherence by controlling the length of the spatial baseline. The graph performs multi-view processing to reduce noise, extracts high-coherence units, and then uses the singular value decomposition method to obtain the least norm least squares solution [16] of the surface deformation rate between image sequences. The detailed technical principle of SBAS is shown in the literature [17].

Suppose that $N+1$ SAR images are acquired in the same place in chronological order (t_1, \dots, t_n) , and at least two images are generated for each short-base subset, and M interferograms can be generated. Meet the following inequalities:

$$\frac{N+1}{2} \leq M \leq M \left(\frac{N+1}{2} \right) \quad \dots (1)$$

It is assumed that the j interferogram is an image generated by t_A and t_B time ($t_B > t_A$). After removing the effects of the ground effect and the terrain phase, the interference phase of any pixel in the interferogram j can be expressed as:

$$\delta\varphi_j = \varphi(t_B) - \varphi(t_A) = \varphi_{def,j} + \varphi_{atmo,j} + \varphi_{flat,j} + \varphi_{noise,j} \dots (2)$$

In the formula, $\sigma(t_B)$ and $\varphi(t_A)$ representing their time phase values, $\varphi_{def,j}$ indicates the deformation phase of the

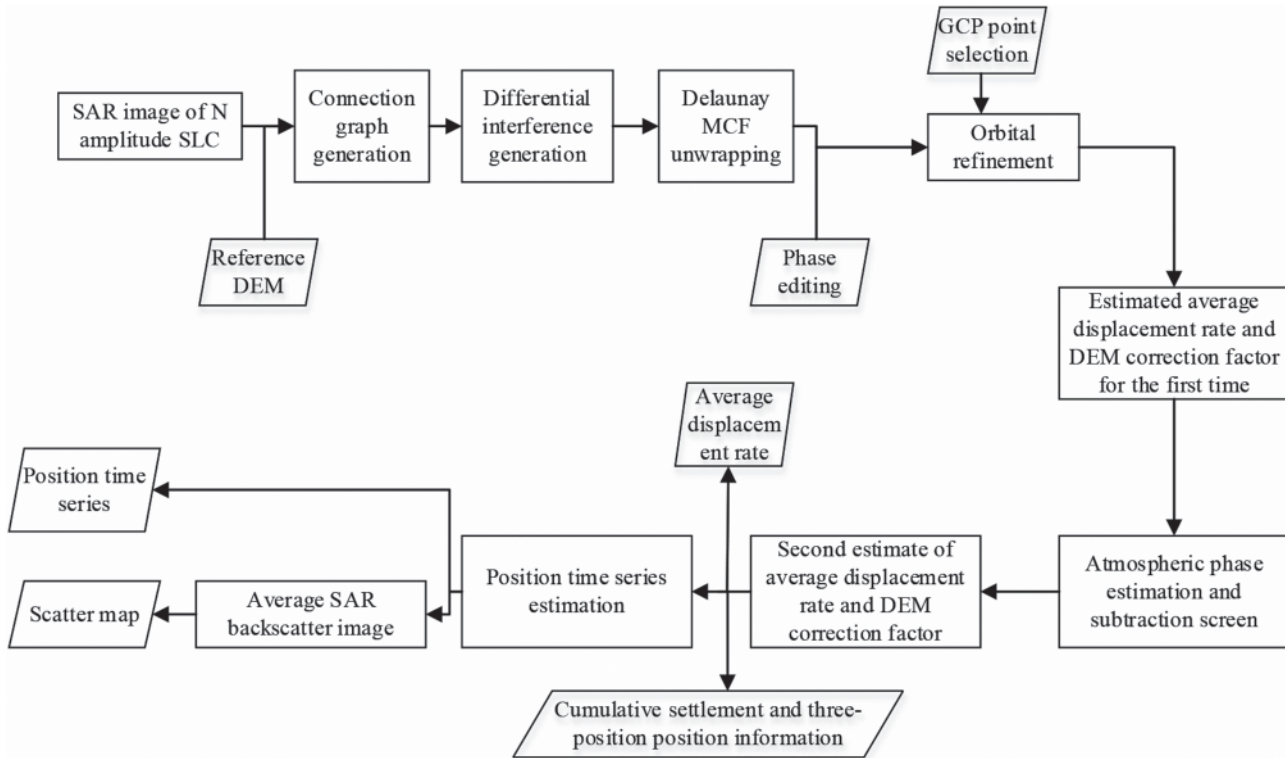


Fig.2 SBAS technical processing flow chart

line of sight to (los), $\varphi_{flat, j}$ represents the residual terrain phase error, $\varphi_{atm, j}$ indicates the atmospheric phase error, $\varphi_{noise, j}$ indicates noise error.

The differential interferometry synthetic aperture radar (D-InSAR) is a combination of interferometric measurement technology and synthetic aperture radar technology. The core idea of the technology is to use the interference phase obtained by repeated orbit observation and remove it twice by differential processing. By observing the common amount [18] (topographic phase, flat phase, atmospheric phase, and noise phase) in the phase, the deformation phase is obtained, and the shape variable is solved according to equation (3).

$$\Delta h = \frac{\Delta r}{\cos\theta} \quad \dots (3)$$

In the middle Δr the settlement value in the direction of the sensor's line of sight, θ the angle of incidence for the sensor.

2.2 DATA PROCESSING

SBAS processing and D-InSAR processing based on SAR scape software. D-InSAR processing mainly includes image registration, de-levelling effect, geocoding, DEM phase difference and other processes to obtain a deformation map. According to the flow shown in Fig.2, the SABS technology mainly includes small baseline combination selection to generate connection graphs, generate differential interferograms, Delaunay MCF unwrapping, select GCP points, linearly estimate displacement rate and DEM correction coefficient, and estimate and subtract the

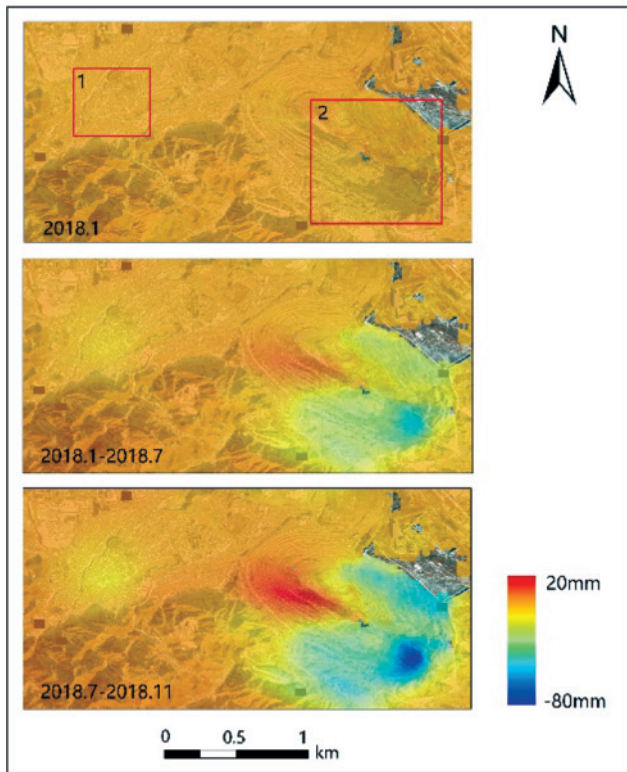
atmospheric phase screen, the total shape variable estimate, and so on.

3. Results and analysis

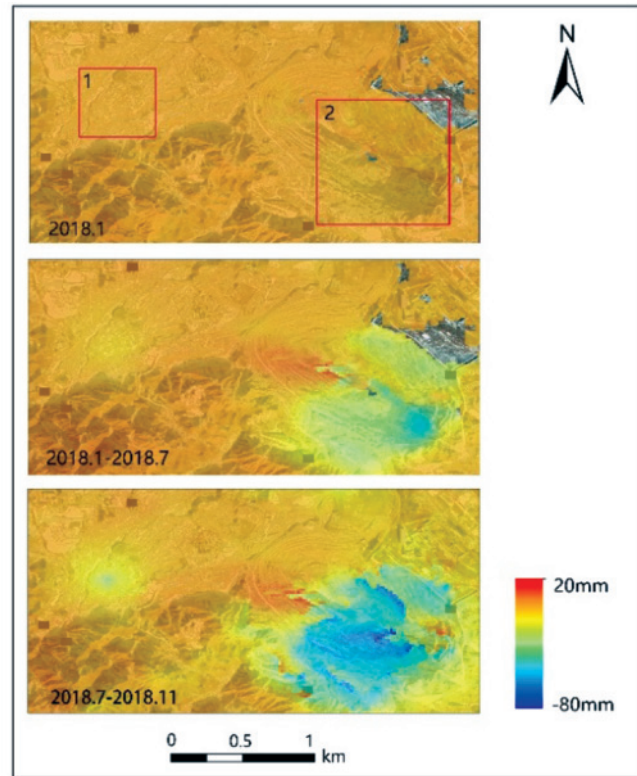
Using the above method, the surface settlement rate was obtained from the study area from January to November 2018 using SBAS technology and sequential D-InSAR technology. In order to more directly understand the surface deformation of the study area, after geocoding in envi, the deformation results are superimposed on Google Image to obtain the settlement map of the mining area (Figs.3 and 3a) is the settlement result of SABS technology, Fig.3(b): For the D-InSAR technology settlement results, this paper uses January 2018 as a reference for the deformation zone. In the Fig.1 is the 5th row of the West 2 mining area, and 2 is the old pit of the open pit; in order to facilitate the observation of the settlement trend of the settlement, The settlement funnel center was selected in the 1 and 2 regions for timing analysis. The results are shown in Fig.4. The deformation rate maps are obtained by D-InSAR and SABS techniques respectively (Figs.5 and 6). From the above results, it can be seen that there are obvious sedimentation funnels in the 1 and 2 regions, and the funnel. The range is increasing and the settlement strength is continuously increasing.

3.1 ANALYSIS OF SURFACE SETTLEMENT OF 5-7 ROWS IN THE WEST 2 MINING AREA

It can be seen from Figs.3 and 4 that the whole west mining area is relatively stable from January to November



(a) SBAS



(b) D-InSAR

Fig.3 Cumulative settlement results

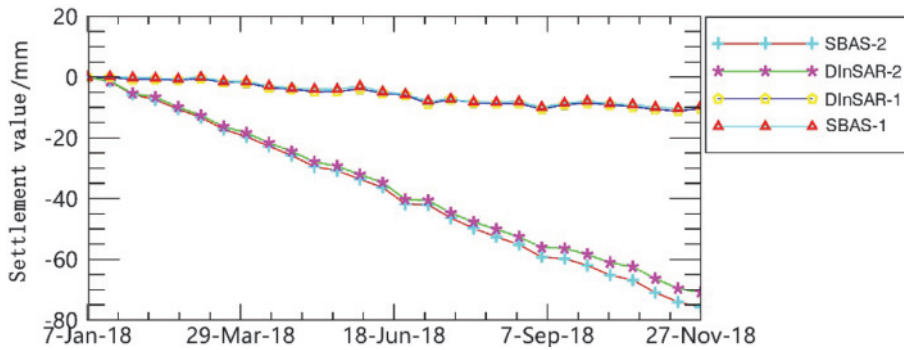


Fig.4 Cumulative settlement curve

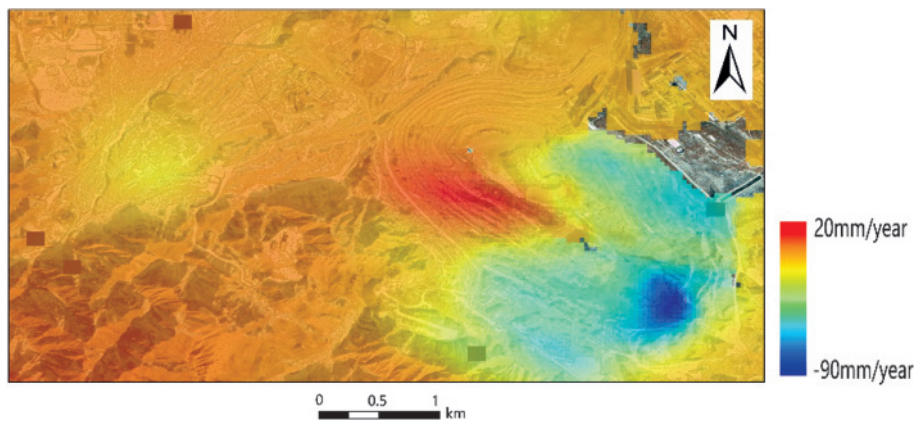


Fig.5 Sedimentation rate map (SABS)

2018. The maximum settlement of this area is 11mm using the time series DInSAR method, and the annual average maximum settlement rate is -14mm/year. The part of the settlement funnel is obviously ranging from 3 mm to 13 mm, and the settlement area is calculated to be about 0.4 km² in combination with arcgis. Compared with the SBAS method, the maximum settlement is 13mm, the annual average maximum sedimentation rate is -14mm/year, the settlement range is between 1mm and 14mm, and the settlement area is 0.45km². After the stoppage, the results of the two methods showed that there was still a slow subsidence in this area in 2018. According to China's deformation monitoring benchmark, the maximum surface settlement per day is 30mm^[19], indicating that lines 5-7 meet the safety standards and can be used for complex mining.

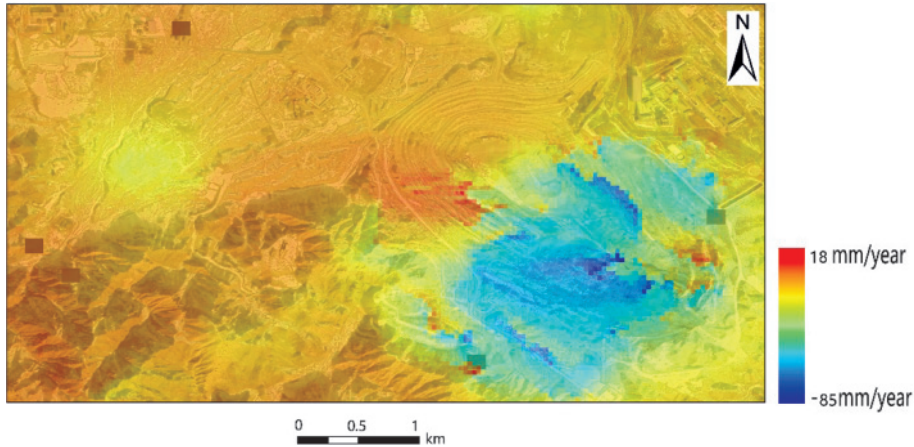


Fig.6 Settlement rate chart (D-InSAR)

3.2 ANALYSIS OF GROUND SETTLEMENT IN OLD PITS

It can be seen from Fig.3 that there is obvious settlement in the southeast part of the old pit. Compared with the 5-7 rows, the settlement area is large, mainly due to the rainwater erosion near the slope, and the settlement is accompanied by landslide. It is obtained based on the time series D-InSAR method. The maximum settlement is 75mm, the maximum settlement rate is -83mm/year, and the settlement area is about 1.4km². The maximum settlement of the SBAS method is 78mm, and the maximum settlement rate is -85mm/year, and the settlement area is 1.37km². The experiment found that there was a slight uplift in a small part of the northwestern part of the old pit. The annual lift was about 20mm. The site saw a slight uplift on the slope, while there were landslide marks in the southwest and slight subsidence in the north of the old pit.

4. Conclusion

Based on the D-InSAR method and the SBAS method, the Sentinel-1A derailment and up-track imagery was used to monitor the surface subsidence of the Jinchuan copper-nickel mining area from January to November 2018. Through two methods, it is found that the surface of 5-7 rows in the second mining area is relatively stable. In the past year, the maximum settlement is 11-13mm, and the maximum settlement rate is -14mm/year. The old pit area has landslide phenomenon, the largest. The settlement is 75-78mm and the maximum sedimentation rate is -85mm/year. The monitoring results of the two methods are similar. It also verifies that the two methods can be used in sparsely planted areas and provide a favorable basis for safe mining in Jinchuan copper-nickel mine.

References

[1] Huang Fei, Huang Lun, Yang Tao, Yang Kai, Wang Man, He Jianbo.(2019): Dynamic variation characteristics of mining subsidence induced by coal

mining face in Longtan Mine [j]. *Mining Safety and Environmental Protection*, 46 (02): 103 -106+110.

[2] Tong Yunwei, Huang Yan, Chen Yu, Tan Wei, OuDepin, Han Fushun. (2019): Time and space analysis of surface subsidence monitoring in D-In SAR mining area [J/OL]. *Surveying and Mapping Science*, 1-10 [2019-05-23].

[3] Maowei Ji, Xiaojing Li, Shunchuan Wu, Yongtao Gao, Linlin Ge. (2011): Use of SAR interferometry for monitoring

illegal mining activities: A case study at Xishimen Iron Ore Mine[J]. *Mining Science and Technology (China)*, 21(6).

[4] Li Deren, Liao Mingsheng, Wang Yan. (2004): Permanent scatterer radar interferometry technology [j]. *Journal of Wuhan University (Information Science Edition)* (08): 664-668.

[5] Chen Deliang, Lu Yanyan, Jia Dongzhen. (2018): Study on Surface Deformation Monitoring in Changzhou Based on StaMPS-InSAR[J]. *Yangtze River*, 49(12):59-65.

[6] NIEBingqi. (2018): Research on landslide deformation detection and hidden danger identification based on InSAR [D]. *Chengdu University of Technology*.

[7] Zhao Jiarui, Ke Changqing. (2019): Monitoring of flow rate of Antarctic Songdao Glacier based on Sentinel-1 SAR data[J]. *Journal of Glaciology and Geocryology*, 41(01):12-18.

[8] Guo Xin, Zhao Yinxi. (2018): Monitoring of Flood Inundation in Ningxiang City, Hunan Province Based on Sentinel-1A SAR[J]. *Remote Sensing Technology and Application*, 33(04):646-656.

[9] Massonnet D, Rossi M, Carmona C, et al. (1993): The displacement field of the Landers earthquake mapped by radar interferometry[J]. *Nature*, 364(6433): 138.

[10] Tomás R, Márquez Y, Lopez-Sanchez J M, et al. (2005): Mapping ground subsidence induced by aquifer overexploitation using advanced Differential SAR Interferometry: Vega Media of the Segura River (SE Spain) case study[J]. *Remote Sensing of Environment*, 98(2-3): 269-283.

[11] Herrera G, Tomás R, Vicente F, et al. (2010): Mapping ground movements in open pit mining areas using differential SAR interferometry[J]. *International Journal of Rock Mechanics and Mining Sciences*, 47(7): 1114-1125.

(Continued on page 551)